IEEE Access
Multidisciplinary | Rapid Review | Open Access Journal

Received 9 September 2022, accepted 21 September 2022, date of publication 26 September 2022,
date of current version 10 October 2022.

Digital Object Identifier 10.1109/ACCESS.2022.3209381

RESEARCH ARTICLE

Optimization Analysis of Full Life Cycle Energy Efficiency Multi-Objective Parallel Pump Sets

QIANG GAO, JIAOLONG XUE, AND HONGWEI YAN, (Member, IEEE)
School of Mechanical Engineering, North University of China, Taiyuan 030051, China

Corresponding author: Qiang Gao (gaoqiang@nuc.edu.cn)

This work was supported in part by the Shanxi Provincial Research Grant Program for Returning Students under Grant 2020-110, and in part by the Shanxi Postgraduate Innovation Program under Grant 2021Y588.

ABSTRACT Aiming at the problem that the current single-objective control model of parallel pumping groups only focuses on the optimization of energy efficiency of operating conditions and operating costs, and cannot adjust the real-time working conditions of the pump group according to the comprehensive energy efficiency state of the pump group in the whole life cycle and adjust the pump group operation strategy accordingly, A multi-objective optimal control model for energy efficiency of a pump set is proposed, which can adjust the weight coefficients of three objective functions autonomously according to the current energy efficiency state of the pump set in the whole life cycle. In this way, the high energy efficiency of the parallel pump group in the low wear stage, that is, the low target deviation and specific energy consumption, and the high reliability in the high wear stage, that is, the lower impeller load improves the efficiency of the pump group in the whole life cycle and extend the service life of the pump group. Determine the multi-objective energy efficiency optimization control model of the pump group, use the main function linear and geometric weighting method, the ideal point value, and the distance deviation method to determine the objective function, and solve the multi-objective ideal point model with the help of LINGO, and obtain the optimal solution of the highest system total efficiency, the lowest pump group specific energy consumption and the highest system reliability. Pareto Frontier Comparison is used to study the transversality of the ideal point model solution set. Experimental results show that through the distribution of the model solution in the indicator space, the model can adjust the control strategy according to the real-time state of the pump group by adjusting the target weight combination.

INDEX TERMS Parallel pumping groups, energy efficiency optimization, full life cycle, multi-objective.

I. INTRODUCTION

Pumping stations are used worldwide in commercial, industrial and residential applications as a tool for fluid distribution [1] and [2], consume about 20% of the world's electricity every year [3]. Centrifugal pumps are the most popular pumping equipment, producing from 80 - 90% of total water treatment [4]. Most medium and large centrifugal pumps offer 65 (or even less) - 85% rated efficiency [5]. Therefore, the energy efficiency of pumping systems has always been a hot topic for researchers [6] and [7]. Today's growing energy market and increasing energy costs require pumping technology to provide new solutions to improve energy efficiency [8]. Many studies published in the field of fluid distribution in recent years have addressed the energy efficiency of multi-pump systems [9]. Some of the researchers use efficiency as the main quality indicator [10]. At the same time, however, maintenance and repairs also account for a large part of the life cycle cost of a pump set. These are all affected by the reliability of the pump.

Parallel pump sets are often used to achieve this goal when large, high or wide flow regulation is required. When parallel pump sets are used, the life cycle cost of all components of a pumping station can be significantly reduced compared to a single pump unit of the same rated power [11] and [12]. Therefore, it is necessary to study the energy efficiency of the parallel pump set during the whole life cycle. To improve the energy efficiency of a multi-pump speed

The associate editor coordinating the review of this manuscript and approving it for publication was Chong Leong Gan.

regulation system, Viholainen *et al.* proposed a throttling and speed control strategy for a multi-pump system based on flow estimation [3]. Koor *et al.* proposed a novel algorithm to reliably predict the operation of parallel control pumps in multi-pump systems [13]. Ahmed *et al.* studied a system with 5 parallel pumps to compare power consumption under different situations [14]. Pandey *et al.* considered the optimization of energy consumption for three parallel pumps without speed regulation [15]. Jia *et al.* considered the optimization of energy consumption in a system consisting of 7 different types of parallel pumps [16]. Luo *et al.* compared the energy consumption of the three pumps with different frequency converter numbers [17]. Spike *et al.* compared the energy consumption of pump systems with 2-4 parallel pumps without speed regulation [18].

To improve the reliability and efficiency of the system, Peng *et al.* optimized the operation of the multi-pump system and studied the feasibility of the optimal control strategy by using genetic algorithms [9]. Wang *et al.* consider the energy-saving control strategy of six parallel pumps, each with a variable speed drive (VSD) [19]. The results show that the asynchronous distributed optimal control algorithm is more effective than the synchronous optimal control algorithm. In summary, in the multi-pump system, a variable speed drive is the most energy-efficient solution for each pump. By adopting different optimization methods, a large number of different control strategies are proposed, which illustrates the complexity and necessity of considering a large number of parameters when optimizing the energy consumption of multi-pump systems.

However, the above articles only focus on the energy efficiency of the multi-pump systems and only consider improving the energy efficiency of the parallel pump systems, without considering their reliability. Zhounian *et al.* used genetic algorithms to optimize single-pump units to improve their reliability [20]. However, it is not taken into account that the optimization criterion is only the maximum service life of the pump unit; The possibility of a trade-off between reliability and energy consumption is not considered. Shiels *et al.* compared the efficiency and reliability of single-pump units and double-pump units, and the results showed that in the latter case, both electricity costs and maintenance costs would be greatly reduced [21]. Oshurbekov *et al.* proposed a trade-off method for tuning a system with only one frequency converter for three parallel pump groups (multi-pump single-drive system). Taking into account the typical duty cycle of a pumping system with variable flow requirements, the proposed method is compared with traditional regulation, and the results show that the proposed compromise method can ensure sufficient reliability in the operation of a multi-pump system without significantly increasing energy consumption [22]. Oshurbekov *et al.* conducted an energy consumption analysis of two pump systems operating in parallel while considering reliability constraints, and the results showed that the proposed balanced control method could minimize the total life cost of the parallel pump system when considering the energy cost and maintenance cost [23].

At present, the common single-objective control models such as the highest efficiency, the lowest power, and the smallest flow deviation of the parallel pump set only focus on the energy efficiency optimization of operating conditions and operating costs, and cannot adjust the operation strategy according to the comprehensive energy efficiency state of the pump set in the whole life cycle. This paper proposes a multi-objective energy efficiency optimization control model for pump sets that can independently adjust the weight coefficients of three objective functions according to the current energy efficiency status of the pump set in the whole life cycle. To achieve the high energy efficiency of the parallel pump group in the low wear stage and high reliability in the high wear stage, the parallel pump group can adjust the control strategy according to the real-time state of the pump group by adjusting the target weight combination, improve the efficiency of the pump group in the whole life cycle and extend the service life of the pump group.

II. PUMP GROUP MULTI-OBJECTIVE ENERGY EFFICIENCY OPTIMIZATION CONTROL MODEL

The experiment is based on two CDLF4-100FSWSC pumps connected in parallel with a water supply platform. the centrifugal pump parameters are shown in Table 1. Under variable speed conditions, the efficiency graph of the rated working condition provided by the pump manufacturer is not very accurate, and the efficiency graph at variable speed needs to be determined. Fig. 1 shows the efficiency diagram of the CDLF4-100FSWSC type pump at variable speed, and Fig. 2 shows the test environment of the laboratory centrifugal pump water supply platform. The valve was used to adjust the centrifugal pump flow rate, and the head and power at rated speed were recorded. After 10 iterations of experimentation, the average value was taken to compare with the curve provided by the manufacturer. The results were shown in Figures 3 to 6. In FIG. 3, the deviation of the actual curve exceeds the flow tolerance when $Q \leqslant 0.35$L/s, and exceeds the flow and head tolerance when $Q \geqslant 1.25$L/s. In FIG. 4, the experimental curve exceeds the flow and power tolerance when $Q \leqslant 0.2$L/s, and exceeds the flow tolerance when $Q \geqslant 1.3$L/s. In FIG. 5, the experimental curve exceeds the flow tolerance when $Q \geqslant 1.1$L/s. Q in this article and Q in all figures in the text are the flow rates of centrifugal pumps. The centrifugal pump in 10 years of use in certain wear, flow, head, power, and efficiency has exceeded the allowable value of the national standard, so the estimation can not be directly applied to the factory curve.

In Fig. 1, the pump characteristic curves at 50Hz, 40Hz, 30Hz, and 20Hz are shown. Within this speed regulation range, the pump conforms to similar laws and can maintain high efficiency. The white dotted line is an equal efficiency curve. On the dotted line, the operating efficiency at different frequencies is approximately the same. The solid white line is the trend line of actual efficiency, which has a certain

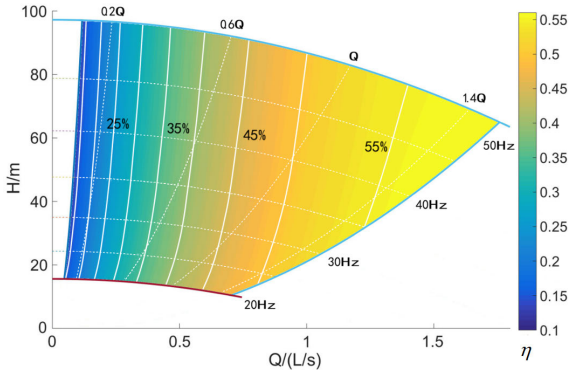

FIGURE 1. Change speed efficiency diagram of CDLF4-100FSWSC, the efficiency curve of this type of pump at different speeds can be observed at 50HZ, 40HZ, 30HZ and 20HZ.

FIGURE 2. Centrifugal pump water supply platform, the various parameters of the centrifugal pump are monitored under this platform.

error compared with the dashed line, but the changing trend of efficiency is the same. Although the pump is designed so that the optimal efficiency point is as close as possible to the rated operating point $Q0$, Figure 1 shows that the maximum efficiency point of the centrifugal pump is not the rated operating point $Q0$, but $1.5Q0$. Excessive pursuit of high efficiency at this time may cause an overload of the motor, so the flow limit is $1.5Q0$ here. The centrifugal pump characteristic curve Q-H can be fitted with a power function, such as Eq. (1):

$$H = a - b \cdot Q^{\lambda} \tag{1}$$

wherein, H and a are the current head and off the head of the centrifugal pump, m; b, λ is the fitting coefficients; Q is the current flow rate, m^3/s.

At present, there are 4 commonly used control methods for parallel pump sets, namely start-stop control, frequency conversion speed regulation, throttle control, and bypass valve control [24]. According to the recommended working area corresponding to the indicators of efficiency, energy consumption, and life, the available control methods of the centrifugal pump system are studied. After determining the structure of the control system, a multi-objective model of the centrifugal pump system that coordinates multiple indicators will be established in combination with the recommended working area, so that the system can dynamically adjust the weights of each indicator according to the current operating

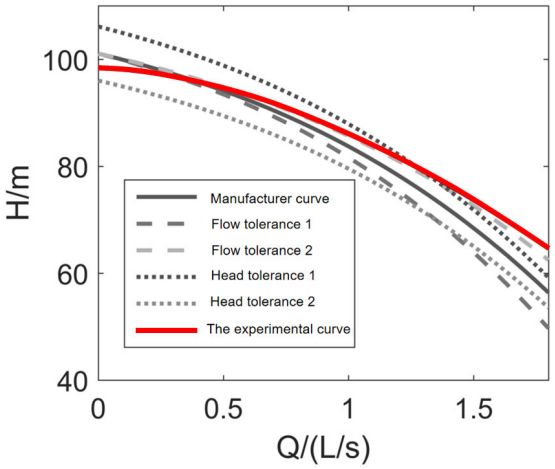

FIGURE 3. Comparison of Q-H curves. The flow rate of the centrifugal pump will have a certain allowable error. The error hovers evenly between positive and negative values. Flow tolerance 1 and flow tolerance 2 are the curves given by the manufacturer. Similarly, head tolerance 1 and head tolerance 2 are also curves given by the manufacturer.

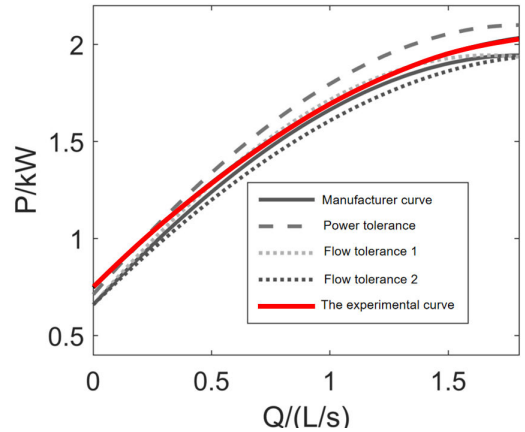

FIGURE 4. Comparison of Q-P curves.

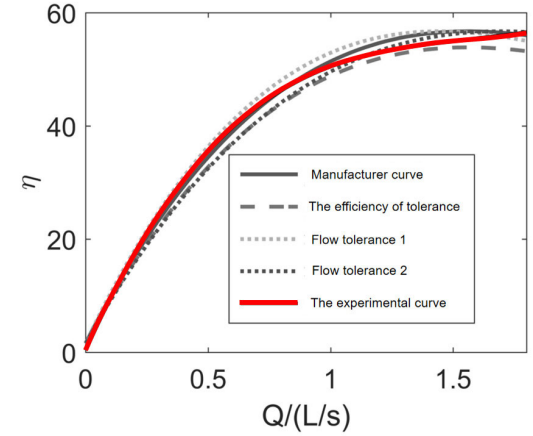

FIGURE 5. Q-η curve comparison.

state and operating objectives, and achieve comprehensive optimization of system operation to reduce the operating cost of the pump group in the whole life cycle. Taking the system in Fig. 6 as the object to study the impact of the control mode on the system.

TABLE 1. Related parameters of parallel centrifugal pump system.

Centrifugal pump model	Rated flow (m3/h)	Rated head (m)	Power(kW)	Revolving speed (rpm)
CDLF4-100FSWSC	4	81	1.67	2900

All kinds of parameters collected in this experiment need to use various sensors, whose main role is to collect various dynamic variables needed in the process of the experiment to ensure real-time monitoring of the data of the experimental platform. In this experiment, the main performance parameters to be tested and the sensors used in the experiment are introduced as follows:

1)Pressure: In the centrifugal pump performance test experiment, pressure is the most important test parameter, each pipeline pressure can be more intuitive to reflect the real-time running state and work performance. Therefore, the test of pressure parameters in this experiment is crucial, and every detail needs to be strictly checked. The sensor used in this experiment is SUP-P300, diffused silicon pressure transmitter, which adopts an imported high-precision and high-stability pressure-sensitive chip. The test range is 0-40mpa, and the accuracy is 0.5.

2)Speed and torque: in the performance experiment of centrifugal pump, the test data of speed and torque are also very necessary. The speed of the centrifugal pump will directly affect the pressure and flow in the performance test experiment of the centrifugal pump. In addition, the normal operation of other components in the experiment is also affected by the speed of the centrifugal pump. Therefore, the speed and torque affect the normal operation of the experiment. In this experiment, the performance of the centrifugal pump can be judged by combining the two parameters of speed and torque. The speed and torque sensors used in this experiment are JN-DN rotary (dynamic) torque sensors, which are divided into torque measurement and speed measurement. Its test range is 500N.m, the test accuracy is 0.5%.

3)Flow rate: In this experiment, the pipeline flow rate is also a very important experimental parameter. As one of the important reference data of centrifugal pump performance, the flow rate needs to be measured accurately in the experiment. In this experiment, there is a certain relationship between the flow rate and the speed pressure, and so on. Ensuring the real-time and accurate monitoring of the flow rate is the premise to ensure the performance test of the centrifugal pump. The flow sensor used in this experiment is MIK-DN100 liquid turbine flow sensor. A turbine flowmeter is a rate meter, which has the characteristics of high accuracy, few moving parts, high-pressure resistance, wide measurement field, small pressure loss, and easy maintenance. Its test range is 0.2-1.2m3/h, and the test accuracy is 1%.

Select two CDLF4-100FSWSC centrifugal pumps in parallel and analyze the single pump and parallel pump groups at 25Hz and 50Hz, respectively, please see Fig. 4, where P1-P5 is the 5 target conditions for the flow rate of 0.5 to 2.5L/s on the pipe network curve, of which P1 is selected as the representative working condition of the high wear stage and P5 is the representative condition of the low wear stage.

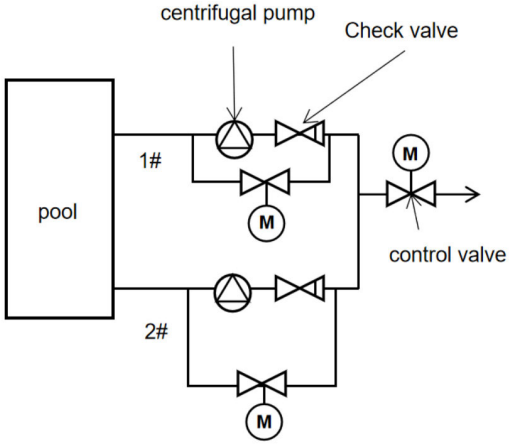

FIGURE 6. Parallel centrifugal pump system, this paper is based on this system to study the control mode of the centrifugal pump, and then study the various parameters of the centrifugal pump.

Comparison of the characteristics of various control methods for centrifugal pumps [25] and [26]. As shown in Table 2.

In summary, each of these three control modes has different advantages and disadvantages, to optimize the control system as much as possible, none of these three control methods can be safely neglected, so the control system of the parallel pump group is initially a combination of three control modes under the parallel connection of the same type of centrifugal pump.

III. CONTROL MODEL SOLVING AND OPTIMIZATION

A. OBJECTIVE FUNCTION

The solution of multi-objective models is complex and generally simplifies calculations by converting to a single-target model. In the whole life cycle of the parallel pump group, to make the centrifugal pump system remain efficient and reliable after adding other targets, the system should be able to adjust the weight coefficients of each target in real-time, so the main target method is excluded. We use the ideal point method. The specific performance of the control strategy from energy efficiency optimization to reliability optimization is as follows: as the wear of the pump unit increases, the solution of the current target is selected from the solutions of the ideal point model. Since the parallel system of the same model is optimal in the equalization of the flow rate, the target operating conditions are evenly divided, and the pump group control optimization is simplified to the

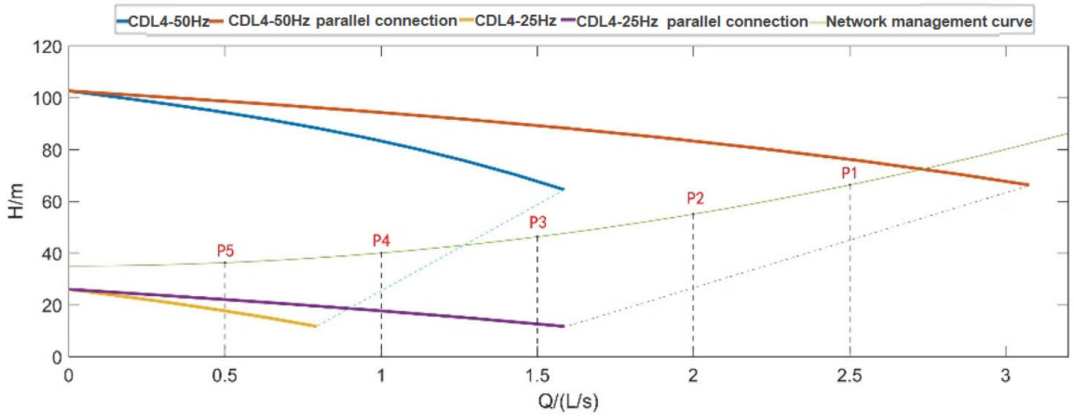

FIGURE 7. Working range of frequency conversion speed regulation of parallel pump units. The CDL4-50Hz in the figure refers to the characteristic curve of this type of single pump at 50Hz, the CDL4-50Hz parallel connection in the figure refers to the characteristic curve of the parallel connection of the two pumps of this model at 50Hz, the CDL4-25Hz in the figure refers to the characteristic curve of the single pump of this type at 25Hz, and the CDL4-25Hz parallel connection in the figure refers to the characteristic curve of the parallel connection of the two pumps of this model at 25Hz. Where P1-P5 is the 5 target conditions for the flow rate of 0.5 to 2.5L/s on the pipe network curve, of which P1 is selected as the representative working condition of the high wear stage and P5 is the representative condition of the low wear stage. Where 0.5-2.5 is evenly distributed.

TABLE 2. Comparison of control modes of parallel centrifugal pumps of the same model.

Control method	Frequency control of motor speed	Throttle control	The bypass control
Adjustable range	Large	Middle	Little
Efficiency	High	Low	Low
System features	Simple	Simple	Simple
Energy efficiency	High	Low	Low
Characteristics	Stepless regulation along the pipe network curve	Changing pipe network characteristics	Control the flow of the main loop when ensuring head

optimization of single pump control. The objective function of the multi-objective control model, such as Eqs. (2):

$$\begin{cases} \min\left[\alpha \cdot Dsys + \beta \cdot Des + \theta \cdot Dre\right] \\ D_{sys} = \dfrac{Q_m \cdot H_m - Q_n \cdot H_n}{Q_n \cdot H_n} \\ D_{es} = \left|\dfrac{E_s - E_{s\min}}{E_{s\min}}\right| \\ D_{re} = \left|\dfrac{F - F_{\min}}{F_{\min}}\right| \end{cases} \tag{2}$$

wherein, α, β, and θ is the weight coefficients of the total efficiency of the system, the specific energy consumption, and reliability of the centrifugal pump, wherein, $\alpha + \beta + \theta = 1$ D_{sys}, D_{es}, and D_{re} are the relative numerical deviations of the total efficiency of the system (the current working condition of the pump from the target working condition), the optimal specific energy consumption condition, and the best reliability; the main loop flow rate provided by Q_m for the single centrifugal pump; H_m is the current pump head; Q_n and H_n are the target conditions of the single centrifugal pump; E_{smin} and F_{min} are the ideal specific energy consumption and the ideal impeller load, respectively. The ideal impeller load is the minimum load that the impeller needs to bear if the pump set meets the current water supply requirements.

B. CONSTRAINTS

1) TARGET CONDITION CONSTRAINTS

The parallel pump system of the same model is approximately equal to the working conditions of each centrifugal pump at maximum efficiency, as shown in Eq. (3):

$$Q_A = \sum_{i=1}^{n} X_i \cdot Q_n = N \cdot Q_n \tag{3}$$

where Q_A is the total target flow rate; i is the centrifugal pump number, $1 \le i \le n$; Xi is the start-stop state of the i centrifugal pump, starting is 1, otherwise 0; N is the total number of centrifugal pumps started.

When the total target flow rate is known, the target head can be solved according to the pipe network curve, and the pipe network curve or pipe network curve parameters are unknown according to the actual working condition point of the centrifugal pump, such as Eqs. (4):

$$\begin{cases} H_n = H_A = d + e \cdot Q_A^2 \\ e = \dfrac{H_{m2} - H_{m1}}{N_2^2 \cdot Q_2^2 - N_1^2 \cdot Q_1^2} \end{cases} \tag{4}$$

wherein, d is the static head, m; e is the drag coefficient of the pipe network; Q_1, H_{m1}, N_1 and Q_2, H_{m2}, and N_2 are the flow, head, and several starts of the single centrifugal pump in the

main loop at different times. Among them, the relationship between the main loop flow, head, and centrifugal pump flow of the single centrifugal pump is as shown in Eqs. (5):

$$\begin{cases} Q_m = Q + Q_{by} \\ H_m = s^2 \cdot a - b \cdot Q_m^2 \end{cases} \tag{5}$$

In the formula, Q_m and Q_{by} are the total flow rate and bypass flow of the single centrifugal pump, respectively; s is the speed regulation ratio, which is about equal to the speed ratio.

To meet the target operating conditions, a single centrifugal pump needs to meet certain constraints, such as Eqs. (6):

$$\begin{cases} H_m \geq H_n \\ Q \geq Q_n \end{cases} \tag{6}$$

2) RECOMMENDED WORKSPACE CONSTRAINTS

Centrifugal pump operating flow rate should be higher than the minimum return flow Q_{min}, when the centrifugal pump flow is too large will lead to motor overload and rapid attenuation of the flow rate, so it is necessary to set the flow constraint; when the frequency is lower than 20Hz, the head error measured by the frequency converter will be increased, and the centrifugal pump can not pump the liquid relatively reliably, you need to set the frequency constraint, such as Eqs. (7). The constraints on specific energy consumption and impeller load change with the operating strategy and are not considered here.

$$\begin{cases} Q_{\min} \leq Q_m \leq \sqrt{\dfrac{H_m}{c}} \\ \left(\dfrac{20}{50}\right) \leq s \leq 1 \end{cases} \tag{7}$$

where c is the coefficient of fit for the efficiency curve of the centrifugal pump $1.5Q_0$.

3) COMPUTE CONSTRAINTS

Since the system contains throttling and bypass control, additional constraints need to be added to avoid poor solutions, such as Eqs. (8):

$$\begin{cases} e = \dfrac{H_m - d}{N^2 \cdot Q^2} \geq e_0 \\ 0 \leq Q_{by} \leq Q_{by\max} \\ Q_{by\max} = \sqrt{\dfrac{H_m}{f}} \end{cases} \tag{8}$$

where d is the same as in Eqs. (4); e_0 is the resistance coefficient of the main loop without throttling control; Q_{bymax} is the highest bypass flow rate under the current operating conditions; f is the resistance coefficient when the bypass valve is fully open.

C. SOLVE THE MODEL

The weight setting of the total efficiency of the system, the specific energy consumption, and the reliability of the system will greatly affect the selection of the optimal solution, and the choice of its value can be determined through the experimental results. This study sets the number of pump sets as n = 2.To study the effect of the weight combination on the results, the value range of the weight coefficients is [0.1, 0.8], and the optimal working conditions under 36 weight combinations are studied at 0.1 intervals, and the target working conditions (Q_A, H_n) is the above P1(2.5, 66.25), P3 (1.5, 46.25) and P5 (0.5, 36.25) above.

To simplify the model, make E_{smin} and F_{min} in Equation 2 the globally optimal values, resulting in Model 1. Using the LINGO solution, the optimal solution for different operating conditions is obtained as shown in Fig. 8(*i*). In Model 1, the solution is the same for different combinations of weights under P1 and P3, and the weight coefficients are invalid. P1 adopts a combination of frequency conversion and bypass control; P3 adopts a combination of frequency conversion and throttling control, P3 is close to but beyond the operating range of the single centrifugal pump, and the system increases the head by increasing the system resistance, and the flow rate meets the demand. The results are ideal at P5, with the increase of the α, the flow rate gradually approaches the ideal flow value under P5 conditions, and as the β and θ increase, the flow tends to be less than the specific energy consumption and impeller load, thus achieving high energy efficiency of the parallel pump group in the low wear phase (lower target deviation and specific energy consumption).

Possible causes of unsatisfactory results in P1 and P3: non-convex functions under P1 and P3, and models with multi-objective to single-objective transformation are unsolvable; E_{smin} and F_{min} use global optimality, and global optimality cannot be achieved under P1 and P3, while the ideal point of total efficiency of the system can be reached. Therefore, let E_{smin} and F_{min} be the optimal values at the same head, that is, the local optimal, to get Model 2. The optimal solution for different operating conditions is shown in Fig. 8 (*ii*). Model 2 is a big improvement over Model 1. Under P1, α increases the solution toward P1 and the number of different solutions increases. The number of different solutions under P5 increases, and the flow is smoother, but the P3 solution remains unchanged, so the model should be considered an improvement.

D. MODEL IMPROVEMENTS

1) THE MAIN FUNCTIONS ARE LINEAR AND GEOMETRICALLY WEIGHTED

Considering that the model is a Mixed-Integer Nonlinear Programming model, the evaluation function is constructed using linear weighting, maximal minimization, and geometric weighting. The following is the objective function of changing models 1 and 2 by geometric weighting to obtain models 3 and 4, such as Eq. (9):

$$\min \left[Dsys^{\alpha} + Des^{\beta} + Dre^{\theta} \right] \tag{9}$$

where α, β, θ are positive coefficients. $\alpha + \beta + \theta = 1$

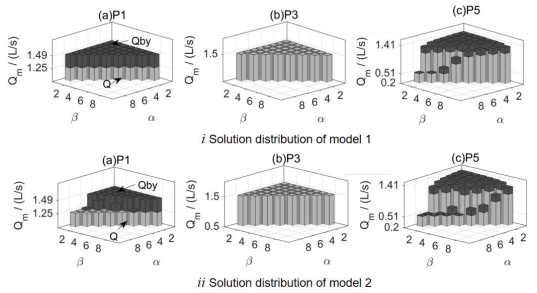

FIGURE 8. Solution distribution of Models 1 and 2.

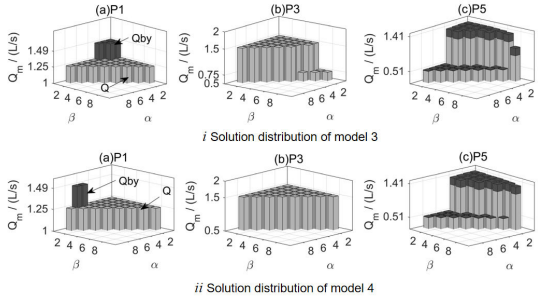

FIGURE 9. Solution distribution of Model 3 and 4.

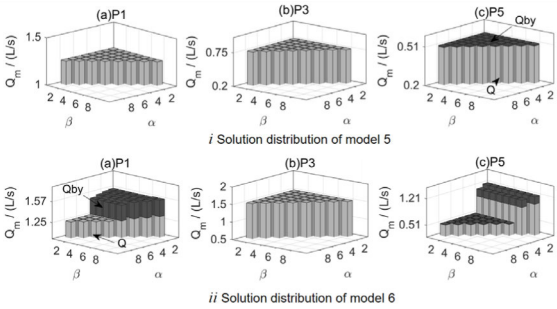

FIGURE 10. Solution distribution of Model 5 and 6.

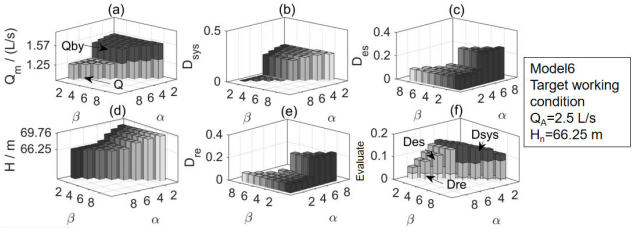

FIGURE 11. Index distribution of Model 6 under P1. (a)–(f) Corresponding parameter changes of model 6 under the P1 working condition, analyzes the number and distribution of model solutions, and concludes that simply narrowing the range gap of D_{sys} and other parameters do not increase the weight coefficient's influence.

We solve again, and the result is shown in Fig. 9. Fig. 9 (i) The distribution of the solutions of model 3 in P1 and P5 is between model 1 and 2, while a solution tending to the total efficiency of the system appears under P3, and in the Figure, the solution that tends to the total efficiency of the system corresponds to a low α value and a wrong trend. Fig. 9(ii) Model 4 also has an erroneous trend in P1, and the distribution of the solution under P3 and P5 is not as good as model 1, so the result of geometric weighting is confusing and unusable.

2) IDEAL POINT VALUES AND DISTANCE DEVIATIONS

To further narrow the numerical gap of each indicator, replace the numerical deviation with the deviation of the centrifugal pump condition from the ideal point, and obtain models 5 and 6, and the objective function is as shown in Eqs. (10):

$$\begin{cases} D_{sys} = \sqrt{\left(\frac{Q_m - Q_n}{Q_n}\right)^2 + \left(\frac{H_m - H_n}{H_n}\right)^2} \\ D_{es} = \sqrt{\left(\frac{Q_m - Q_{es}}{Q_{es}}\right)^2 + \left(\frac{H_m - H_{es}}{H_{es}}\right)^2} \\ D_{re} = \sqrt{\left(\frac{Q_m - Q_{re}}{Q_{re}}\right)^2 + \left(\frac{H_m - H_{re}}{H_{re}}\right)^2} \end{cases} \tag{10}$$

wherein, Q_{es}, H_{es}, Q_{re}, h_{re} is the working conditions of the rational points of energy consumption and reliability, respectively. The solution result is shown in Fig. 10.

In Fig. 10 (*i*), Model 5 has only one solution at P1-P5, which is not in line with the actual operating conditions; in Fig. 10 (*ii*), the distribution of model 6 solutions is similar to model 2, but the number is reduced. Overall, the performance of distance deviation is inferior to numerical deviation. The distance deviation has a significant effect on narrowing the range gap between parameters such as D_{sys}, as shown in Fig. 11, the corresponding parameters of model 6 under P1 conditions, at which point the number and distribution of solutions in models 5 and 6 should be better than those of models 1 and 2. Therefore, simply narrowing the range gap between parameters such as D_{sys} does not increase the influence of the weight factor.

IV. PARETO FRONTIER OF MULTI-OBJECTIVE MODELS

Two questions arise in the discussion of the above model: whether the function under P3 is non-convex, and why narrowing the range gap for indicators such as D_{sys} does not increase the influence of the weight coefficient. To do this, we solve the multi-objective model directly.

The multi-objective model is converted to a single target by a weighted combination, and its weight combination can be understood as the orientation of the face that approximates the Pareto frontier [27], as shown in Fig. 12:

In the plot, changing the ratio of α to β changes the direction of the approximation curve to get the individual solutions on the Pareto frontier (such as point A), but when there is a nonconvex region in the Pareto frontier, changing the weights does not find all solutions of the nonconvex region (such as point B), which is easy to fall into local optimality. In this case, the unidentified model cannot do anything about it.

There are generally two solutions to solve such problems, one is to estimate the range of the optimal solution set, solve it after equidistant points, and then select the non-dominant solution from the resulting solution set to form an approximate solution set of Pareto solution sets; the other is to use evolutionary algorithms such as genetic algorithms, particle swarm algorithms, etc. for global random search. However, when there are too many goals, the workload of the first method is huge, and the scope of the subjective judgment

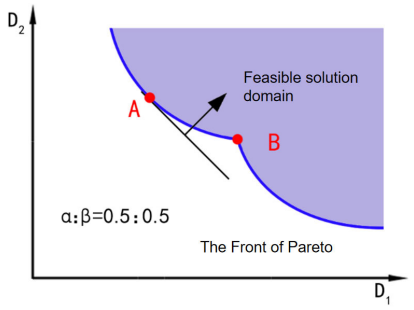

FIGURE 12. Pareto front and weight.

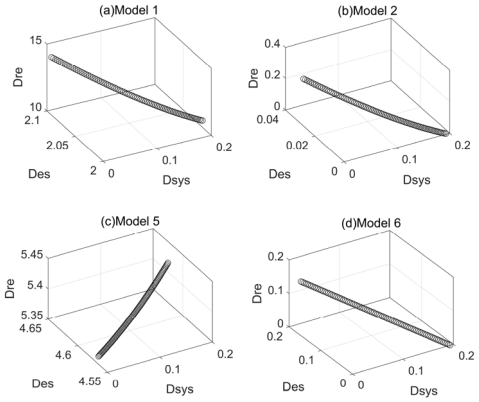

FIGURE 13. Pareto front under P1.

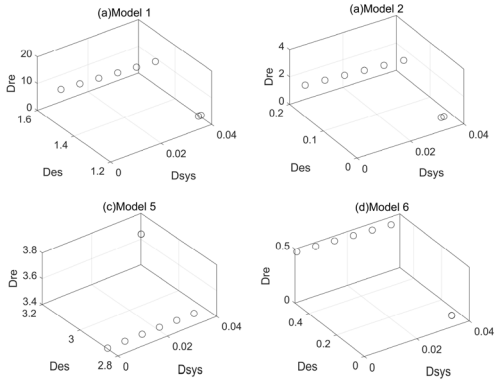

FIGURE 14. Pareto front under P3.

of the optimal solution is likely to be biased, so the second scheme is used here.

A. PARETO FRONTIERS UNDER DIFFERENT EVALUATION FUNCTIONS

Since this problem is a typical mixed-integer nonlinear programming problem, the multi-objective particle swarm algorithm is used to calculate the Pareto frontier of the single-target model based on the solution sets of each model obtained above [28], [29]., as shown in Figs. 13 to 15.

In Fig. 13 c, the edge of the Pareto frontier is facing the coordinate origin, while the single-target model approaches the Pareto frontier from the origin, so no matter how much the weight combination is changed, only the solution closest to the origin can be obtained, which explains why Model 5 narrows the index range gap but performs the worst. Pareto frontier for the remaining models performs normally, but

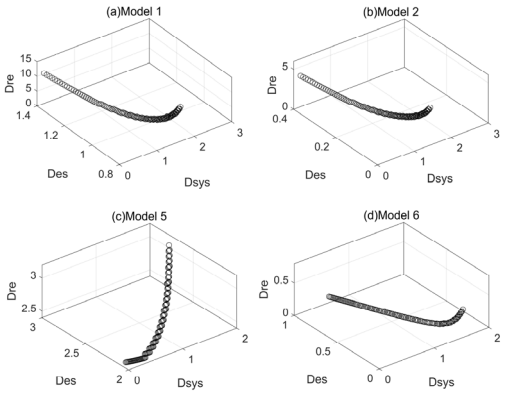

FIGURE 15. Pareto front under P5.

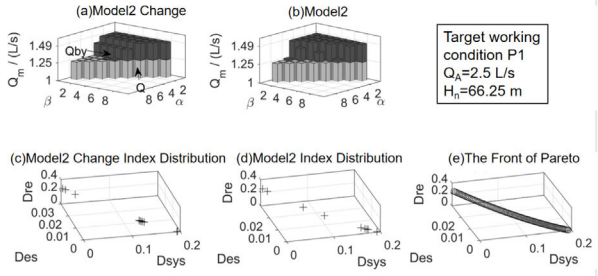

FIGURE 16. Comparison of model results under P1.

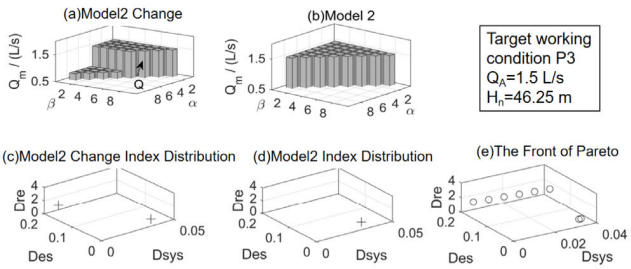

FIGURE 17. Comparison of model results under P3.

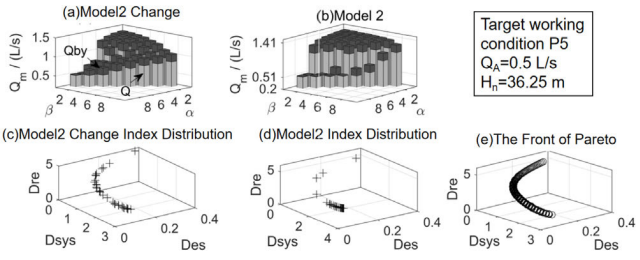

FIGURE 18. Comparison of model results under P5.

model 6 has a low curvature, is close to a straight line, and tends to have uneven solution-set distributions when approximately.

In Fig. 14, the Pareto leading edge of Model 5 is located opposite to the other model positions, with the solution set at N 1 being completely obscured, while the Pareto leading edge at N taking 2 is parallel to the D_{sys} axis, resulting in only the solution at the minimum of D_{sys} being approximated. The curves of the remaining models are similar, but they all get only the solution of N out of 1, which is in the lower right corner.

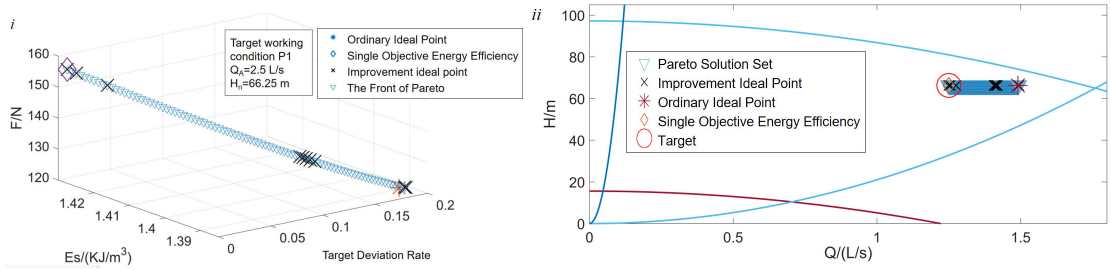

FIGURE 19. Evaluation and distribution of solution set of different models under P1.

The problem with Model 5 in Fig. 15 is the same as in Model 5 in Fig. 13, whereas Model 6 has a lower curvature, so models 1 and 2 have better solution distributions and quantities than Model 6. In summary, Model 2 is the best, but the metric range gap is too large to traverse all the solutions well, so here are improvements for Model 2.

B. MODEL 2 IMPROVEMENTS

Further refinement of the best model above, Model 2. Normalize the evaluation metrics in the objective function, such as Eq 11:

$$\min\left[\alpha\cdot\frac{Dsys}{D_{sys\,\max}}+\beta\cdot\frac{Des}{D_{es\,\max}}+\theta\cdot\frac{Dre}{D_{re\,\max}}\right] \quad (11)$$

where D_{sysmax} is the maximum system efficiency deviation value at the current target, which can be replaced by the system efficiency deviation value at the ideal point of energy consumption and reliability; D_{esmax} and D_{remax} can be obtained at the target operating point.

After solving, it is compared with model 2, and the result is as shown in Figs. 16 to 18: In Fig. 16, the number of different solutions of model 2 and the improved model is comparable, and the solution distribution of model 2 is slightly better, but the difference is not large; in Fig. 17, the improved model obtains a solution with N being 2 and D_{sys} at 0 when the α is small; in Fig. 18, the number and distribution of different solutions of the improved model are significantly better than model 2, and the excessiveness of different solutions is also better. Overall, the improved model is superior to Model 2.

Synthesizing all the above models, it can be found that the transversality of the model to Pareto solution sets mainly depends on the distribution of Pareto frontiers in the evaluation space and the range gap of each index in the objective function. Models such as models 5 and 6 satisfy the second point, but the poor distribution of Pareto frontiers makes the traversal significantly worse than other models, so the structure of the evaluation indicator needs to be paid attention to. Geometry-weighted models 3 and 4 did not achieve a good set of solutions, and the reasons for this need further study.

The solution set evaluation of the improved model is well distributed in the index space, which is a multi-objective control model that can autonomously adjust the target weight according to the current pump group state and achieve adaptive working conditions, which can achieve high energy efficiency of parallel pump group in low wear stage (lower target deviation and specific energy consumption), high reliability in high wear stage (lower impeller load), thereby improving the efficiency of the pump group in the whole life cycle and prolonging the service life of the pump group.

V. COMPREHENSIVE ANALYSIS AND COMPARISON OF MODELS

The improved multi-objective ideal point model is compared with the single-objective energy efficiency model, the common ideal point model, and the ordinary multi-objective model, and the solution set under P1, P5, and P3 targets are distributed in the objective function space and flow head plots as shown in Figs. 19 to Fig. 21.

In Fig. 19(i), the single-target energy efficiency model has only one solution, which is at the lowest target deviation rate; the ordinary ideal point model has only one solution with impeller load and lowers specific energy consumption under variable weights, and the improved multi-objective ideal point model has a solution for intermediate comprehensive targets in addition to the solution at the lowest target deviation rate and the lowest impeller rate, and its lowest distribution set distribution and quantity are inferior to the Pareto solution set of the ordinary multi-target model, but it meets the requirements of multi-objective control and has a fast solution speed. Fig. 19(ii) can be seen in the actual operation of the pump group under different control models of the flow and head output, by changing the weights of each target, the improved multi-objective ideal point model can obtain a different focus of the solution.

In Fig. 20, under the P5 target, the solution of the single-target energy efficiency model is similar to P1; the number and distribution of solutions of the ordinary ideal point model have increased, but are still inferior to the improved multi-objective ideal point model; the gap between the solution set of the improved multi-objective ideal point model and the Pareto solution set is reduced, the solution set is more evenly distributed on the Pareto frontier, and the pump group can transition more smoothly under different control strategies when the weights of each target change gradually.

In Fig. 21, under the P3 target, the single-objective energy efficiency model and the normal ideal point model obtain solutions with N as 2 and N as 1, respectively; the improved multi-objective ideal point model has solutions in both cases, showing the Pareto solution set that is closest to the multi-objective model.

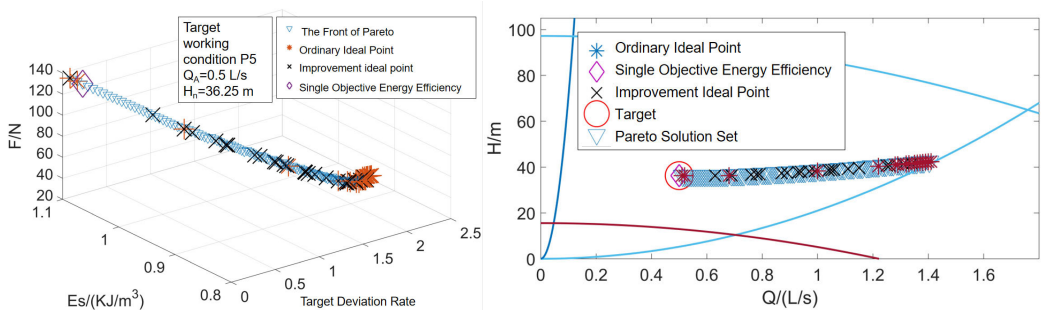

FIGURE 20. Evaluation and distribution of solution set of different models under P5.

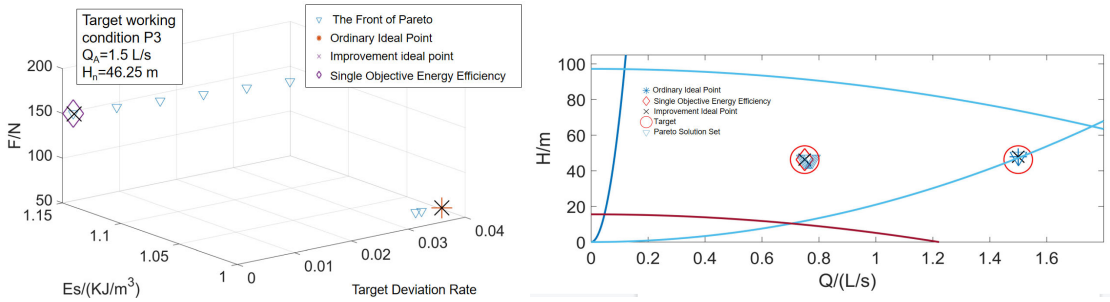

FIGURE 21. Evaluation and distribution of solution set of different models under P3.

TABLE 3. Comparison of different models.

Model category	Solves the speed	Energy efficiency optimization	Reliability optimization	The integrity of the optimal solution set
Single-target energy efficiency model	≤1min	√	×	No
Ordinary ideal-point model	≤10min	√	√	General
Ordinary multi-objective model	≥40min	√	√	Very high
Improve the ideal-point model	≤2min	√	√	High

In summary, the improved multi-objective ideal point model is paired with other models, for example, Table3.

VI. CONCLUSION

This paper aims at the problem that it is currently impossible to adaptively adjust the real-time working conditions of the pump group according to the comprehensive energy efficiency status of the pump group in the whole life cycle and adjust the operation strategy of the pump group accordingly, this paper proposes a method that can be used in the whole life cycle of the pump set according to the current pump set. Multi-objective pump group energy efficiency optimization control model, with three objective function weight coefficients independent adjustment. The following conclusions were drawn:

The combined control mode of frequency conversion, bypass and throttling matching the multi-objective model is determined, the objective function is determined by using the main function linear and geometric weighting method, the ideal point value and the distance deviation method, and the multi-objective ideal point model is solved with the help of LINGO, and the optimal solution of the highest system total efficiency, the lowest pump group specific energy consumption and the highest system reliability is obtained.

Compared with Pareto frontiers, the traversal of the ideal point model solution set is studied, and the optimal model is further improved, so that the model solution set evaluation is better distributed in the index space.

Experiments with different models show that the improved model has the advantages of simple structure, fast solution speed, uniform distribution of solution set under variable weight, and high coverage of Pareto solution set so that the control strategy can match the pump group's whole life cycle more comprehensively. This results in higher energy efficiency (lower target deviation and ratio of energy consumption) in the low wear phase, higher reliability (lower impeller load) in the high wear phase, and higher efficiency of pump group service life.

REFERENCES

[1] B. Nesbitt, *Handbook of Pumps and Pumping*. Amsterdam, The Netherlands: Elsevier, 2006.

[2] I. J. Karassik, J. P. Messina, and P. Cooper, *Pump Handbook*. New York, NY, USA: McGraw-Hill, 2008.

[3] J. Viholainen, J. Tamminen, T. Ahonen, J. Ahola, E. Vakkilainen, and R. Soukka, "Energy-efficient control strategy for variable speed-driven parallel pumping systems," *Energy Efficiency*, vol. 6, no. 3, pp. 495–509, Aug. 2013, doi: 10.1007/s12053-012-9188-0.
[4] J. Tuzson, *Centrifugal Pump Design*. Hoboken, NJ, USA: Wiley, 2000.
[5] P. G. Kini and R. C. Bansal, "Effect of voltage and load variations on efficiencies of a motor-pump system," *IEEE Trans. Energy Convers.*, vol. 25, no. 2, pp. 287–292, Jun. 2010, doi: 10.1109/TEC.2009.2032628.
[6] L. Nelik, *Fundamentals With Applications*. Boca Raton, FL, USA: CRC Press, 1999.
[7] V. Goman, S. Oshurbekov, V. Kazakbaev, V. Prakht, and V. Dmitrievskii, "Energy efficiency analysis of fixed-speed pump drives with various types of motors," *Appl. Sci.*, vol. 9, no. 24, p. 5295, Dec. 2019, doi: 10.3390/app9245295.
[8] V. Vodovozov and Z. Raud, "Predictive control of multi-pump stations with variable-speed drives," *IET Electr. Power Appl.*, vol. 11, no. 5, pp. 911–917, May 2017, doi: 10.1049/iet-epa.2016.0361.
[9] P. Wu, Z. Lai, D. Wu, and L. Wang, "Optimization research of parallel pump system for improving energy efficiency," *J. Water Resour. Planning Manage.*, vol. 141, no. 8, 2015, Art. no. 04014094, doi: 10.1061/(ASCE)WR.1943-5452.0000493.
[10] J. R. Arribas and C. M. V. Gonzalez, "Optimal vector control of pumping and ventilation induction motor drives," *IEEE Trans. Ind. Electron.*, vol. 49, no. 4, pp. 889–895, Aug. 2002, doi: https://doi.org/10.1109/TIE.2002.801240.
[11] Z. Lai, Q. Li, A. Zhao, W. Zhou, H. Xu, and D. Wu, "Improving reliability of pumps in parallel pump systems using particle swam optimization approach," *IEEE Access*, vol. 8, pp. 58427–58434, 2020, doi: 10.1109/ACCESS.2020.2980396.
[12] S. Oshurbekov, V. Kazakbaev, V. Prakht, V. Dmitrievskii, and L. Gevorkov, "Energy consumption comparison of one variable-speed pump and a system of two pumps: Variable-speed and fixed-speed," *Appl. Sci.*, vol. 10, no. 24, p. 8820, 2020, doi: 10.3390/app10248820.
[13] M. Koor, A. Vassiljev, and T. Koppel, "Optimal pump count prediction algorithm for identical pumps working in parallel mode," *Proc. Eng.*, vol. 70, pp. 951–958, Jan. 2014, doi: 10.1016/j.proeng.2014.02.106.
[14] A. Ahmed, B. Moharam, and E. Rashad, "Power saving of multi pump-motor systems using variable speed drives," in *Proc. 20th Int. Middle East Power Syst. Conf. (MEPCON)*, Cairo, Egypt, Dec. 2018, pp. 839–844.
[15] S. Pandey, R. P. Singh, and P. S. Mahar, "Optimal pipe sizing and operation of multistage centrifugal pumps for water supply," *J. Pipeline Syst. Eng. Pract.*, vol. 11, no. 2, 2020, Art. no. 04020007, doi: 10.1061/(ASCE)PS.1949-1204.0000447.
[16] M. Jia, J. Zhang, and Y. Xu, "Optimization design of industrial water supply pump station considering the influence of atmospheric temperature on operation cost," *IEEE Access*, vol. 8, pp. 161702–161712, 2020, doi: 10.1109/ACCESS.2020.3021304.
[17] Y. Luo, Z. Xiong, H. Sun, and Y. Guo, "Research on energy-saving operation control model of the multi-type configuration centrifugal pump system with single invert," *Adv. Mech. Eng.*, vol. 9, no. 7, pp. 1–10, 2017, doi: 10.1177/1687814017707650.
[18] H. Sike, J. Xuejing, and G. Huifen, "Optimization of the number of multiple pumps running simultaneously in open cycle cooling water system in power plant," *Energy Proc.*, vol. 17, pp. 1161–1168, Jan. 2012, doi: 10.1016/j.egypro.2012.02.222.
[19] X. Wang, Q. Zhao, and Y. Wang, "An asynchronous distributed optimization method for energy saving of parallel-connected pumps in HVAC systems," *Results Control Optim.*, vol. 1, Dec. 2020, Art. no. 100001, doi: 10.1016/j.rico.2020.100001.
[20] Z. Lai, P. Wu, S. Yang, and D. Wu, "A control method to balance the efficiency and reliability of a time-delayed pump-valve system," *Math. Problems Eng.*, vol. 2016, pp. 1–10, Jan. 2016, doi: 10.1155/2016/5898209.
[21] S. Shiels, "When two pumps are cheaper than one," *World Pumps*, vol. 1997, no. 372, pp. 58–61, 1997, doi: 10.1016/S0262-1762(99)80210-7.
[22] S. Oshurbekov, V. Kazakbaev, V. Prakht, and V. Dmitrievskii, "Improving reliability and energy efficiency of three parallel pumps by selecting trade-off operating points," *Mathematics*, vol. 9, no. 11, p. 1297, Jun. 2021, doi: 10.3390/math9111297.
[23] S. Oshurbekov, V. Kazakbaev, V. Prakht, and V. Dmitrievskii, "Increasing service life and system efficiency of parallel pumps using combined pump regulation," *Water*, vol. 13, no. 13, p. 1808, Jun. 2021, doi: 10.3390/w13131808.
[24] X. Li, M. Zhu, and J. Xie, "Numerical simulation of transient pressure control in a pumped water supply system using an improved bypass pipe," *Original Sci. Paper*, vol. 10, no. 62, pp. 614–622, 2016, doi: 10.5545/sv-jme.2016.3535.
[25] P. Olszewski and J. Arafeh, "Parametric analysis of pumping station with parallel-configured centrifugal pumps towards self-learning applications," *Appl. Energy*, vol. 231, no. 1, pp. 1146–1158, 2018, doi: 10.1016/j.apenergy.2018.09.173.
[26] P. Olszewski, "Genetic optimization and experimental verification of complex parallel pumping station with centrifugal pumps," *Appl. Energy*, vol. 178, pp. 527–539, Sep. 2016, doi: 10.1016/j.apenergy.2016.06.084.
[27] J. Lee, S.-I. Lee, J. Ahn, and H.-L. Choi, "Pareto front generation with knee-point based pruning for mixed discrete multi-objective optimization," *Struct. Multidisciplinary Optim.*, vol. 58, no. 2, pp. 823–830, 2018, doi: 10.1007/s00158-018-1926-2.
[28] M. A. Mellal and E. Zio, "An adaptive particle swarm optimization method for multi-objective system reliability optimization," *Proc. Inst. Mech. Eng., O, J. Risk Rel.*, vol. 233, no. 6, pp. 990–1001, Dec. 2019, doi: 10.1177/1748006X19852814.
[29] M. S. Hasanoglu and M. Dolen, "Multi-objective feasibility enhanced particle swarm optimization," *Eng. Optim.*, vol. 50, no. 12, pp. 2013–2037, Dec. 2018, doi: 10.1080/0305215X.2018.1431232.

QIANG GAO received the bachelor's degree in fluid transmission and control from the Taiyuan University of Technology and the master's degree in mechanical and electronics from the Taiyuan University of Technology, in 2004. He is currently engaged in teaching and scientific research with the School of Mechanical Engineering, North University of China, mainly engaged in the research of complex mechanical equipment structure optimization and autonomous control, electromechanical and hydraulic system state detection, and intelligent control.

JIAOLONG XUE received the Graduate degree from the School of Mechanical and Electronic Engineering, North University of China, in 2020, where he is currently pursuing the master's degree in mechanical engineering with the School of Mechanical Engineering. He is mainly engaged in the research of mechanical and electrical liquid system status detection and intelligent control.

HONGWEI YAN (Member, IEEE) was born in Taiyuan, Shanxi, China. He received the Ph.D. degree in mechanical engineering from the Taiyuan University of Technology. He is currently an Associate Professor and a master's Supervisor at the School of Mechanical Engineering, North University of China. His research interests include dangerous emergency equipment and prevention and control technology.